# pH-Responsive Membranes from Self-Assembly of Poly[2-(Dimethylamino)ethyl Methacrylate] Brush Silica Nanoparticles

Yulia Eygeris, Noah Ulery, and Ilya Zharov*

*Department of Chemistry, University of Utah, 315 South 1400 East, Salt Lake City, Utah 84112, USA*

**ABSTRACT**: We have prepared novel pH-responsive nanoporous membranes by self-assembly of silica nanoparticles carrying poly[2-(dimethylamino)ethyl methacrylate] (PDMAEMA) brushes with DP in 100-450 range. The nanoparticles were prepared by surface-initiated ARGET-ATRP, and the membranes were assembled by pressure-driven deposition onto porous supports. The permeability and pore size of the resulting robust membranes were studied using water and hexane flux and filtration cut off experiments. The pore size of the PDMAEMA HNP membranes measured by water flux was ca. 22 nm and was mostly independent of the polymer brush length. We attributed this to a combination of PDMAEMA brush swelling and its permeability to water. In contrast, the pore size measured by hexane flux strongly depended on the degree of polymerization. The flux and pore size for these membranes in water strongly depended on pH. The pore size decreased by a factor of 1.6 when changing the pH from neutral to acidic. pH-Responsive HNP membranes combine many attractive properties, including control of filtration cut-off, responsive permeability, and high flux at low pressure. The reversible self-assembly of PDMAEMA HNP membranes may help not only in their facile preparation but also in material recycling if biofouling occurs. The key features of PDMAEMA HNP assemblies are attractive in membrane separations, molecular valves, and biosensors, where the precise control over the pore size and pore gating are highly desirable.

**KEYWORDS**: *nanopore, membrane, permeability, polymer brush, nanoparticle*

## Introduction

The conformation of responsive polymeric chains can be manipulated by changing pH, solvent, temperature, or ionic strength.[1] The incorporation of such chains in porous membranes allows manipulating the pore size, membrane selectivity, and permeability, which are of particular interest in the rapidly developing field of nanofiltration[2] and ultrafiltration.[3] For example, precise control over the size of the nanopores is useful for size-selective separations of a wide variety of solutes, including but not limited to proteins, bacteria, viruses, and even individual ions.[4,5]

Numerous and diverse materials are used in the preparation of nanoporous membranes, with polymer-nanoparticle composites becoming an increasingly popular choice in this area.[6] The polymer part in such composites provides desired functionality and variability in the pore size, while the introduction of inorganic nanoparticles adds physical and thermal stability.[7-9] There are currently two main approaches to prepare such hybrid composites - blending nanoparticles into a polymer matrix or assembling nanoparticles functionalized with the polymer. The latter approach creates homogenous structures through "bottom-up" design, avoiding typical problems of nanoparticle fillers such as particle aggregation.[8] However, even though polymer/nanoparticle composite systems have been around for over 20 years, little is known about the driving forces behind the assembly of polymer-grafted nanoparticles and the properties of the resulting materials.[10,11]

pH-responsive polymers undergo a reversible change in volume, solubility, and conformation in response to changes in pH of the surrounding solution. This property is commonly utilized in drug delivery[12] and fabrication of biomedical devices.[13] For the membrane applications, this means that the responsive brushes inside the nanopores can act as flow valves and filters with gated size selectivity.[14]

Previously, we reported the preparation of responsive membranes by modifying the surface of nanopores in silica colloidal crystals with several different types of responsive polymer brushes, including temperature responsive poly(N-isopropylacryl amide) (PNIPAM)[15] and poly(L-alanine),[16] and pH-responsive poly[2-(dimethylamino)ethyl methacrylate], PDMAEMA.[17] In the latter case, we studied the molecular transport in PDMAEMA-modified nanopores as a function of pH using cyclic voltammetry and diffusion measurements. We observed pH-response that was reversible and the pore size that could be tuned by varying the pH.

More recently, we developed a new approach to the preparation of nanoporous membranes, by self-assembly of polymer brush-grafted "hairy" silica nanoparticles (HNPs).[18] In an attempt to expand this approach to responsive materials, we explored HNPs

carrying responsive polymer brushes as building blocks for responsive nanoporous membranes. In the case of HNP membranes prepared with polyelectrolyte brushes, we observed ionic strength responsive behavior, suggesting that the polymer brushes not participating in HNP particle-particle interactions are free to change their conformation inside the interstitial spaces. Most recently, we reported on the preparation of temperature-responsive membranes using HNPs carrying PNIPAM brushes.[20]

One question that remained unanswered is how the HNP membranes would behave if their polymer brushes were to change from neutral to charged. Such charging would allow controlling the flux through the nanopores of these membranes using pH, but at the same time might result in membrane disintegration due to the repulsive forces between HNPs. To investigate such novel HNP assemblies and to potentially create novel responsive HNP membranes, we decided to use PDMAEMA HNPs as building blocks for the membranes and study their permeability as a function of pH. The results of this work are described below.

## Materials and methods

*Materials*. Anisole, 3-aminopropyltriethoxysilane (APTES), triethylamine, 2-bromoisobutyryl bromide, 2-(dimethylamino)ethyl methacrylate (DMAEMA; was purified using an alumina column before use), 1,1,4,7,10,10-hexamethyl triethylenetetramine (HMTETA). 4-dimethylaminopyridine (DMAP) and tetraethoxysilane (TEOS) were purchased from Alfa Aesar. Dichloromethane (DCM), methanol, ascorbic acid, dimethylformamide (DMF) and ammonia hydroxide solution were purchased from Fischer Chemicals. Copper (II) chloride dihydrate was purchased from Acros. Polystyrene spheres were purchased from Polysciences, Inc.

*Characterization.* Scanning electron microscopy (SEM; FEI Nova NanoSEM 630) and transmission electron microscopy (TEM; JEOL JEM-1400) were used to image the HNPs. Thermogravimetric analysis of polymer-modified particles was conducted using a SSC 5200 thermogravimetric analyzer (Seiko). A Branson 1510 sonicator was used for all sonications. UV/Vis measurements were performed using an Ocean Optics USB4000 instrument.

*Preparation of silica particles.* Silica nanoparticles (SNPs) were prepared using the Stober method.[21] The size of nanoparticles was determined by dynamic light scattering (DLS) to be 226±20 nm and confirmed by TEM. Formed nanoparticles were dried in the vacuum oven for 3 hours at 50 $^{o}$C before further modification.

*Grafting of polymerization initiator moieties.* ATRP sites were prepared through previously described procedures in two steps.[17,20] In the first step, primary amines were grafted on the surface to facilitate the addition of initiator sites as follows: 1 mL of APTES was added to a suspension of approx. 2 g of Stöber silica particles in 15 mL of dry acetonitrile. The reaction flask was immersed in a 60$^{o}$C oil bath and stirred for 6 hours. Aminated particles were collected by centrifugation, washed at least three times with acetonitrile and dried. In the second step, polymerization initiator sites were grafted to the surface of the silica particles as follows: to a prepared suspension of 1 g of aminated silica particles in 50 mL anhydrous DCM added 40 mg (0.3 mmol) of DMAP, 2.09 mL (15 mmol) of triethylamine and 1.61 mL (13 mmol) of 2-bromoisobutyryl bromide. The reaction was left stirring at room temperature for 24 hours. Resulting particles were collected by centrifugation, washed at least three times with DCM and then dried. Successful surface modification after each step was confirmed using thermogravimetric analysis (TGA).

*Polymerization.* Polymer brushes were grafted through activators regeneration by electron transfer atom-transfer radical polymerization (ARGET-ATRP).[22] In a typical polymerization run, 500 mg of silica with initiator sites was combined with 6.5 mL (38.5 mmol) DMAEMA in 2.4 mL anisole and 50 µl of $CuBr_2$and HMTETA (1:10 molar ratio, respectively, with $CuBr_2$ concentration of 200 mM) solution in DMF. Then, the reaction mixture was degassed by two freeze-pump-thaw cycles and 8 mg (45 µmol) ascorbic acid in 1 ml DMF was added to the mixture. The reaction was stirred at 60 ˚C under a nitrogen atmosphere, with polymer length controlled by allowed reaction time. Formed "hairy" particles were collected by centrifugation, washed at least three times with acetonitrile and dried. The degree of polymerization was calculated based on the TGA data, using a polymer grafting density of 0.3 $nm^{-2}$ which results from this reported procedure.[23]

*Membrane preparation.* 10 mL dead-end filtration cells (Sterlitech Corporation and Millipore Amicron) were used to prepare and study the HNP membranes. A membrane layer was prepared through pressure-driven deposition of a suspension of ~2 mg of nanoparticles in 10 mL 50% acetonitrile/water at neutral pH onto a nylon support with a nominal pore size of 0.22 µm (Tisch Scientific, North Bend, OH; pore size determined using bubble point method). The applied pressure for all measurements was set to 1 bar.

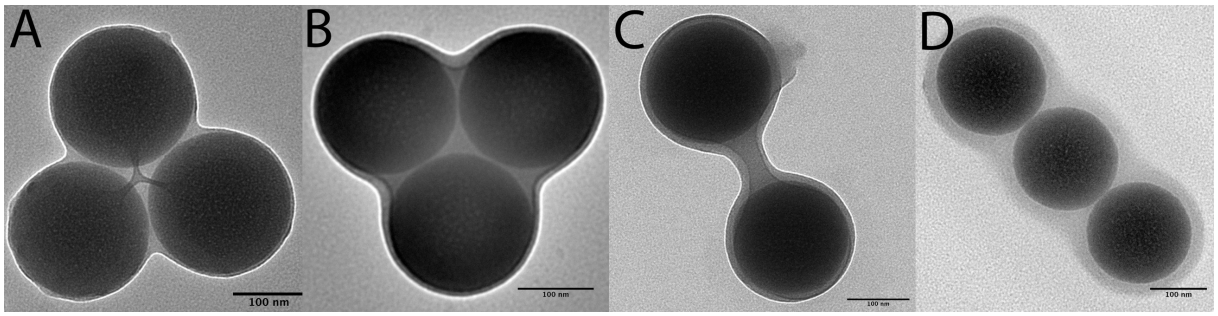


***Figure 1.*** *TEM micrographs of PDMAEMA HNPs: (A) DP=100, (B) DP=250, (C) DP=350, (D) DP=450. Scale bars are 100 nm.*

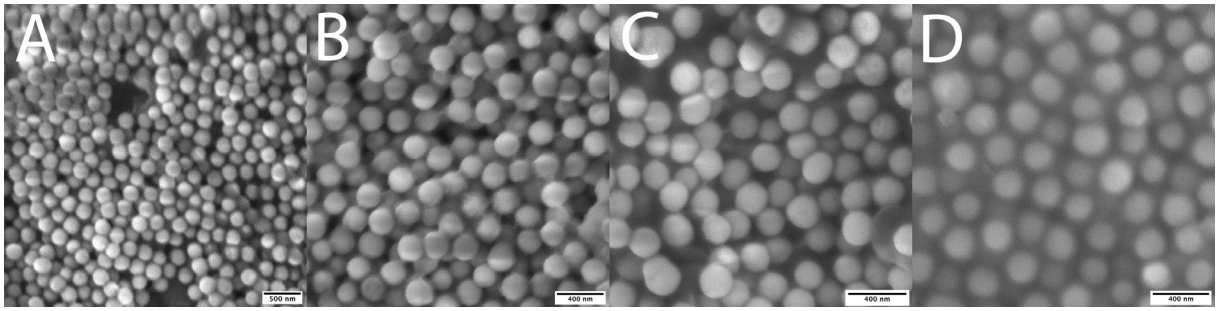


***Figure 2.*** *SEM top-view micrographs of PDMAEMA membranes: (A) DP=100, (B) DP=250, (C) DP=350, (D) DP=450. Scale bars are 500 nm (A) and 400 nm (B-D).*

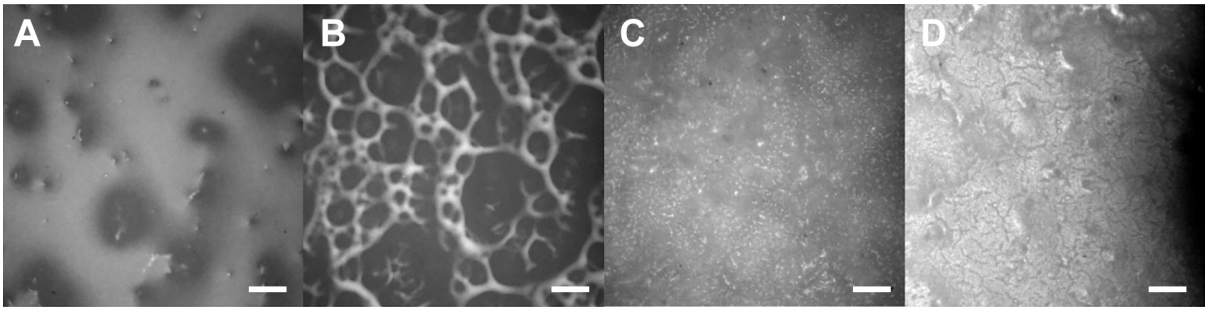


***Figure 3.*** *Micrographs of PDMAEMA membrane (DP=450) drying over time: (A) min, (B) 1 min, (C) 5 min, (D) 10 min. Scale bars are 10 μm.*

*Membrane testing.* Water with the nominal resistivity of 18 MΩ∗cm was used in the preparation of all solutions and water flow experiments. Water, 1 M HCl and hexanes flow were measured by driving the solvent through the membrane and weighing collected fractions over time. The pore size cutoff was determined using polystyrene spheres suspension in water (50 μL of 0.2% by weight solution further diluted with 4 mL of water; polystyrene sphere sizes were 15, 30, 50, and 100 nm in diameter). The solution was driven through the membrane, and the amount of the permeate was determined spectrophotometrically at a wavelength of 240 nm.

## Results and discussion

### Preparation of PDMAEMA Particles

Stober silica particles were functionalized with polymerization initiator moieties in two steps as reported earlier.[17] The diameter of the silica particles (230±20 nm) was determined by DLS and confirmed by TEM. pH-responsive PDMAEMA polymer brushes were grafted from the silica surface using surface-initiated atom-transfer radical polymerization (SI-ATRP) as shown in Scheme 1. The polymer length was controlled by the reaction time, with the shortest polymer formed within 30 minutes and the longest polymer within 2 hours. The success of each

polymerization and the degree of polymerization (DP) were determined by TGA using the polymer grafting density of 0.3 $nm^{-2}$.[23] We will refer to the prepared HNPs by their DP of 100, 250, 350 and 450, corresponding to the degree of polymerization.

The polymer length will be important for the further discussion of polymer response inside the pores. It can be estimated using the scaling model, which is widely applied to spherical polymer brushes.[24,25] The model describes the different conformations of polymer brush in terms of the critical distance:

$$R_C = R_0 \sigma^{*1/2} \nu^{*-1} \quad (1)$$

where $R_0$ - particle radius, $\sigma^* = \sigma l^2$ - reduced grafting density ($\sigma$ - grafting density, 0.3 for our system,[23] $l$ - monomer length, 0.25 nm for acrylates), $\nu^* = \nu/(4\pi)^{1/2}$ - reduced excluded volume parameter ($\nu$ - excluded volume parameter). Depending on the relationship between the critical distance and particle radius, at a given distance from the particle surface the polymer may exist in either semi-dilute (relaxed) or concentrated (stretched) conformation regime, or a combination of these two.[26] Based on the scaling model, the prepared PDMAEMA brushes should exist in concentrated regime, therefore the prepared brush length h can be estimated as $l \times DP^{0.8}$ and thus it varies from ca. 10 to 36 nm.

TEM images of individual PDMAEMA HNPs (Figure 1) demonstrated the presence of the polymer brush and confirmed that the polymer length increases with the reaction time, resulting in a thicker polymer shell. This result is consistent with the previously published reports.[27-29] Based on the collected micrographs, we anticipated that the DP=450 will have the highest polymer filling inside the pores formed by the interstitial spaces between the HNPs, although this prediction was not observed experimentally (see below).

## Preparation and Properties of PDMAEMA HNP Membranes

The "hairy" particles were assembled into the membranes by pressure-driven deposition onto porous nylon supports from 1:1 acetonitrile-water suspension of HNPs at neutral pH. The solvent composition was chosen to maximize the solubility of the "hairy" particles. The average membrane thickness was 50 microns.

We imaged the membranes by SEM to investigate their morphology (Figure 2). The top-view micrographs reveal a similar trend to that observed in the TEM micrographs of the corresponding HNPs

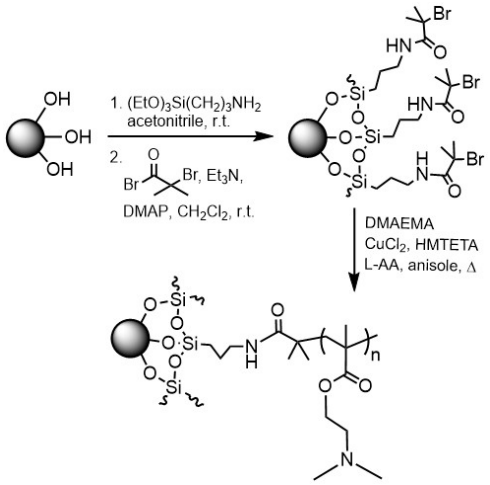


***Scheme 1.*** *Preparation of PDMAEMA polymer-brush silica nanoparticles.*

- the polymer coating is increasingly more prominent with increasing polymer length.

While TEM and SEM provide important information about the HNP membranes, this imaging is performed under a high vacuum. Since polymer brushes are extremely sensitive to the surrounding media, imaging in vacuum does not present the membrane state under ambient conditions. Therefore, we imaged the membranes in the air in the presence of water using optical microscopy and recorded the dynamic drying behavior of the HNP membranes (Figure 3).

The DP=450 PDMAEMA HNP membrane appearance changes dramatically as the membrane dries out confirming the drastic effect of the environment on the polymer brush swelling. At the beginning of the image acquisition, the membrane appears amorphous, with no distinct particle features. We speculate that the wet swollen brushes smooth out the membrane surface. After one minute, the polymer begins to dry, forming long strands across the membrane surface. We observed polymer strands connecting the HNPs on a much smaller scale in the SEM micrographs (best seen in Figure 1A and 2B). While the scale is different, we believe these observations are related to the same phenomenon. At the five-minute mark, the membrane is dry but structurally intact, but its thickness is reduced, indicating the polymer brush collapse. After ten minutes, small cracks begin to appear. To the best of our knowledge, this is the first reported instance of recording the polymer brush drying process, and this experiment once again emphasizes the importance of the brush environment, as the brushes may change their thickness from over 110 nm (wet) to ca. 20 nm (dry, from TEM micrographs, Figure 2D). It is

important to note that the membranes could be cycled between dry and wet states numerous times without the loss of functionality in terms of their permeability under the aqueous conditions.

## PDMAEMA HNP Membrane Permeability

Water flux at neutral pH for PDMAEMA HNP membranes with different polymer brush length is shown in Table 1. The flux for all prepared membranes is at the lower end of the typical range of 5-200 L/m²h at 1 atm reported for commercial ultrafiltration membranes.[30] We calculated membrane permeabilities $\kappa$ as defined by Darcy's law:

$$\kappa = \frac{J\mu L}{\Delta P} \quad (2)$$

where $J$ - flux, $L$ - thickness (on average approx. 45 μm), $\Delta P$ - applied pressure, $\mu$ - the viscosity of water. From there, we estimated the effective pore size using the Kozeny-Carman equation, commonly applied to describe fluid flow through a bed of packed particles:

$$R_{KC}^2 = 4K\kappa/\varepsilon \quad (3)$$

where $\varepsilon$ is the porosity of the system, 36% for randomly packed spheres,[31] and $K$=*4.8* is Kozeny constant.[32]

The permeability of the membranes did not depend significantly on the polymer brush length, with the effective pore diameter of ca. 22 nm for all DPs (Table 1). It must be noted, however, that the Kozeny-Carman equation often underestimates the pore size compared to the experimental filtration cut-offs due to the slip flow phenomenon when the hydrophobic interactions between the water and the silica surface create a smaller effective volume for the fluid to pass through.[33- 37] To further confirm the effective pore size, we tested the filtration cutoff using polystyrene spheres of different sizes. We found that the membranes retained 30 nm polystyrene spheres (retention factor of 92±5%) but were permeable to 15 nm spheres (retention factor of 12±4%), in general agreement with the pore sizes calculated using the water flow measurements.

We believe that the observed pore size is the result of the interplay between the polymer brush thickness and the interdigitation of the polymer chains, with the additional effect of water transport through the swollen polymer brush. The first two effects can be semi-quantitatively described using the hard-sphere-soft-shell percolation model of HNP packing developed earlier by us.[31] Based on the equations we developed, the HNPs with the shortest PDMAEMA brush (DP=100) pack with ca. 50% interdigitation of the brushes. Indeed, randomly packed spheres (volume fraction of 0.64) with 230 nm hard core and soft shell of 10 nm would produce membranes with effective pore diameter of ca. 62 nm if no interdigitation occurred, and the reduction of the pore diameter to 22 nm would result from ca. 50% shell overlap. If the polymer brush thickness increased without the change in the overlap, the effective pore size would also increase. Since the pore size remained nearly constant for the membranes made with longer polymer brushes, the overlap between the brushes must have increased to reach ca. 80% for DP=450, as would be expected for the longer polymer chains in more relaxed conformations.

Our results for PDMAEMA HNP membranes suggest that the degree of interdigitation depends on the polymer composition and charge. For example, for the PNIPAM HNP membranes made using a similar silica core (247 nm) and DP of 80, 250 and 450, the pore diameter was 30, 20 and 10 nm, respectively,[20] which is similar to that for the

***Table 1.*** *Water flux through PDMAEMA HNP membranes at neutral pH and pH 1 and corresponding permeability and effective pore diameter.*

| DP | Membrane parameters | | |
|---|---|---|---|
| | **parameter** | **pH 7** | **pH 1** |
| **100** | $J$, L/m²h | 18±4 | 7±3 |
| | κ, nm² | 2.3±0.5 | 0.8±0.3 |
| | $D_{KC}$, nm | 22±2 | 13±3 |
| **250** | $J$, L/m²h | 11±1 | 7±1 |
| | κ, nm² | 1.8±0.3 | 1.2±0.2 |
| | $D_{KC}$, nm | 20±2 | 16±1 |
| **350** | $J$, L/m²h | 29±7 | 10±1 |
| | κ, nm² | 2.5±1.2 | 0.8±0.3 |
| | $D_{KC}$, nm | 23±5 | 13±3 |
| **450** | $J$, L/m²h | 18±5 | 7±2 |
| | κ, nm² | 2.3±0.9 | 0.9±0.3 |
| | $D_{KC}$, nm | 22±4 | 14±2 |

***Table 2.*** *Hexane flux through PDMAEMA HNP membranes and corresponding permeability and effective pore diameter.*

| **DP** | $J$, $10^2$ L/m²h | **κ, nm²** | $D_{KC}$, **nm** |
|---|---|---|---|
| **100** | 18±2 | 70±9 | 122±8 |
| **250** | 13±2 | 66±14 | 119±13 |
| **350** | 7±1 | 18±8 | 62±14 |
| **450** | 0.05±0.01 | 0.2±0.1 | 7±1 |

PDMAEMA HNP membranes. In contrast, for HNP membranes made using polyelectrolyte copolymer brushes with DP of 100, 350 and 500 (267 nm silica core), the pore diameters were 99, 65 and 32 nm, respectively.[19] Thus, it appears that mostly neutral polymer brushes, such as PNIPAM and PDAMEMA, interdigitate to a similar extent, leading to similar effective nanopore diameters for similar degrees of polymerization (20 nm for DP=250), while charged polyelectrolyte brushes interdigitate to a smaller extent leading to larger effective pore diameters for similar degrees of polymerization.

Additionally, we attribute the relatively high and constant permeability of PDMAEMA HNP membranes in water to the transport through the polymer brush. We tested this hypothesis by comparing the behavior of the membranes in water (a "good" solvent) and in a "bad" solvent, hexane. In water, the polymer brushes are expected to swell and thus contribute to the overall permeability of the pores, thus the calculated pore size is a combination of through-pore and through-polymer transport. In a "bad" solvent, the polymer-polymer interactions should dominate over the polymer-solvent interactions, so the polymer brushes would not be permeable and would block the pores based their degree of polymerization and interdigitation.

The results for the hexane flux measurements are shown in Table 2. The pore sizes determined using hexane flux vary dramatically for membranes with different degrees of polymerization. The largest pore diameter was ca. 122 nm for DP=100 and the smallest pore diameter was ca. 7 nm for DP=450. The decrease in the pore size can be attributed to the pore volume displacement by the polymer due to the preferable polymer-polymer interactions, and, as expected, the extent of displacement is proportional to the degree of polymerization. In a "bad" solvent, strong polymer-polymer interactions produce an essentially nonporous material displacing the volume of the nanopores, while in a "good" solvent the molecular transport can occur through the polymer matrix.[38] Previously, we observed a similar effect for long PNIPAM brushes formed inside silica nanopores.[15] Since the nonpolar solvent flow through the packed array of silica nanoparticles does not experience slip flow, the pore size estimated by the Kozeny-Carman equation is more accurate.[33-37] Therefore, the pore sizes measured using the non-polar, "bad" solvent flux are not affected by the contribution of the permeation through the polymer brushes inside the nanopores and the pore size measured under these conditions is closer to its geometrical meaning.

### PDMAEMA HNP Membrane pH-Responsive Behavior

PDMAEMA is a pH-responsive polymer that swells under acidic conditions due to the presence of the tertiary amine groups in the polymer side chains. The $pK_a$ of PDMAEMA is 7.0-7.5,[28,29] therefore, at pH < 7 the PDMAEMA brushes become protonated and swell, and thus in HNP assemblies the portions of the brush not participating in the interdigitation should extend further into the volume of the nanopores. The extent of this swelling may be attenuated by the confinement of the polymer chains inside the HNP assemblies. Indeed, we previously reported a significantly lower $pK_a$ of 4-5 for PDAMEMA chains formed inside silica nanopores.[38] In HNP assemblies, the confinement effect would be less pronounced compared to that inside solid nanopores, but it may nevertheless play a role in reducing the protonation of the chains and their swelling.

Water flux at neutral and low pH for PDMAEMA HNP membranes with different polymer brush length is shown in Table 1. The average pore diameter for all membranes, determined by water flux, decreased from ca. 22 nm to ca. 13 nm once HCl was introduced, a factor of ca. 1.6. Apparently, the PDAMEMA polymer length had little effect on pore size response to pH. This is different from our previous observations where longer polymer brushes showed a smaller flux change for polyelectrolyte HNP membranes[19] and for PNIPAM HNP membranes.[19] However, it is consistent with the pore size behavior as a function of the polymer length for the PDMAEMA HNP membranes described above. Importantly, the PDMAEMA HNP membranes remained intact under the pH cycling and their physical dimensions did not change, indicating that once assembled, the HNPs are held together strongly by the polymer-polymer interdigitation.

The magnitude of the pore size change we observed (by a factor of 1.6) is consistent with the PDMAEMA brush behavior reported previously. Specifically, PDMAEMA brushes grafted from the flat[39] and spherical[40] surfaces swell on average 1.5 times in response to lowering the pH, as demonstrated by DLS, SLS, and ellipsometry, with the brush length on the surfaces having no significant effect on the magnitude of the response.

## Conclusions

We demonstrated that "hairy" PDAEMA HNPs assemble into stable nanoporous membranes. whose pore size responds to pH. The pore sizes in these membranes, measured using the water flux, were similar to those measured for the previously

reported PNIPAM NHP membranes, but show little dependence on the degree of polymerization of the PNIPAM brush. no dependence on the degree of polymerization. We attribute this to the high degree of PDMAEMA swelling and to its partial permeability for water. In contrast, the pore size in hexane showed a strong dependence on the degree of polymerization, supporting the above notion. PDMAEMA brushes, when protonated at acidic pH, further swell into the interstitial spaces between the nanoparticles, thus partially blocking the pores. The pore size decreased 1.6 times in response to the change in pH from 7 to 1, which is typical for PDMAEMA brushes in solution.

pH-Responsive HNP arrays combine many attractive properties, including control of filtration cut-off, responsive permeability, high flux at low pressure, and resistance to biofouling. The reversible self-assembly of HNP membranes may help not only in their facile preparation but also in material recycling if biofouling occurs. The key features of PDMAEMA HNP assemblies are attractive in membrane separations, molecular valves, and biosensors, where the precise control over the pore size and pore gating are highly desirable.

## Author information

**Corresponding Author**
*Email: i.zharov@utah.edu

**Notes**

The authors declare no competing financial interest.

## Acknowledgements

This work was supported by the National Science Foundation (CHE-1710052). Dr. Thang Quoc Tran (Chemical Engineering Department at the University of Utah) collected optical microscope images.

## References

1. Dai, S.; Ravi, P.; Tam, K. C. PH-Responsive Polymers: Synthesis, Properties and Applications. *Soft Matter* **2008**, *4* (3), 435–449.
2. Mohammad, A. W.; Teow, Y. H.; Ang, W. L.; Chung, Y. T.; Oatley-Radcliffe, D. L.; Hilal, N. Nanofiltration Membranes Review: Recent Advances and Future Prospects. *Desalination* **2015**, *356*, 226–254.
3. Kammakakam, I.; Lai, Z. Next-Generation Ultrafiltration Membranes: A Review of Material Design, Properties, Recent Progress, and Challenges. *Chemosphere* **2023**, *316*, 137669.
4. Pendergast, M. M.; Hoek, E. M. V. A Review of Water Treatment Membrane Nanotechnologies. *Energy Environ. Sci.* **2011**, *4* (6), 1946–1971.
5. Adiga, S. P.; Jin, C.; Curtiss, L. A.; Monteiro-Riviere, N. A.; Narayan, R. J. Nanoporous Membranes for Medical and Biological Applications. *WIREs Nanomedicine and Nanobiotechnology* **2009**, *1* (5), 568–581.
6. Zydney, A. L. Chapter 15 - High Performance Ultrafiltration Membranes: Pore Geometry and Charge Effects. In *Membrane Science and Technology*; Oyama, S. T., Stagg-Williams, S. M., Eds.; Inorganic Polymeric and Composite Membranes; Elsevier, 2011; Vol. 14, pp 333–352.
7. van Reis, R.; Zydney, A. Bioprocess Membrane Technology. *J. Membr. Sci.* **2007**, *297* (1), 16–50.
8. Jancar, J.; Douglas, J. F.; Starr, F. W.; Kumar, S. K.; Cassagnau, P.; Lesser, A. J.; Sternstein, S. S.; Buehler, M. J. Current Issues in Research on Structure–Property Relationships in Polymer Nanocomposites. *Polymer* **2010**, *51* (15), 3321–3343.
9. Kumar, S. K.; Benicewicz, B. C.; Vaia, R. A.; Winey, K. I. 50th Anniversary Perspective: Are Polymer Nanocomposites Practical for Applications? *Macromolecules* **2017**, *50* (3), 714–731.
10. Moffitt, M. G. Self-Assembly of Polymer Brush-Functionalized Inorganic Nanoparticles: From Hairy Balls to Smart Molecular Mimics. *J. Phys. Chem. Lett.* **2013**, *4* (21), 3654–3666.
11. Min, Y.; Akbulut, M.; Kristiansen, K.; Golan, Y.; Israelachvili, J. The Role of Interparticle and External Forces in Nanoparticle Assembly. *Nature Mater* **2008**, *7* (7), 527–538.
12. Schmaljohann, D. Thermo- and pH-Responsive Polymers in Drug Delivery. *Advanced Drug Delivery Reviews* **2006**, *58* (15), 1655–1670.
13. Jeong, B.; Gutowska, A. Lessons from Nature: Stimuli-Responsive Polymers and Their Biomedical Applications. *Trends in Biotechnology* **2002**, *20* (7), 305–311.
14. Tokarev, I.; Minko, S. Stimuli-Responsive Hydrogel Thin Films. *Soft Matter* **2009**, *5* (3), 511–524.
15. Schepelina, O.; Zharov, I. PNIPAAM-Modified Nanoporous Colloidal Films with Positive and Negative Temperature Gating. *Langmuir* **2007**, *23* (25), 12704–12709.
16. Abelow, A. E.; Zharov, I. Poly(L-Alanine)-Modified Nanoporous Colloidal Films. *Soft Matter* **2009**, *5* (2), 457–462.
17. Schepelina, O.; Poth, N.; Zharov, I. pH-Responsive Nanoporous Silica Colloidal Membranes *Adv. Funct. Mater.* **2010**, *20* (12), 1962–1969.
18. Khabibullin, A.; Fullwood, E.; Kolbay, P.; Zharov, I. Reversible Assembly of Tunable Nanoporous Materials from "Hairy" Silica Nanoparticles. *ACS Appl. Mater. Interfaces* **2014**, *6* (19), 17306–17312.
19. Eygeris, Y.; White, E. V.; Wang, Q.; Carpenter, J. E.; Grünwald, M.; Zharov, I. Responsive Nanoporous Membranes with Size Selectivity and Charge Rejection

from Self-Assembly of Polyelectrolyte "Hairy" Nanoparticles. *ACS Appl. Mater. Interfaces* **2019**, *11* (3), 3407–3416.
20. Eygeris, Y.; Wang, Q.; Görke. M.; Grünwald, M.; Zharov, I. Temperature Responsive Nanoporous Membranes from Self-Assembly of PNIPAM Hairy Nanoparticles. *ACS Appl. Mater. Interfaces* **2023**, *15*, 29384–29395.
21. Stöber, W.; Fink, A.; Bohn, E. Controlled Growth of Monodisperse Silica Spheres in the Micron Size Range. *Journal of Colloid and Interface Science* **1968**, *26* (1), 62–69.
22. Min, K.; Gao, H.; Matyjaszewski, K. Use of Ascorbic Acid as Reducing Agent for Synthesis of Well-Defined Polymers by ARGET ATRP. *Macromolecules* **2007**, *40* (6), 1789–1791.
23. Cao, L.; Man, T.; Zhuang, J.; Kruk, M. Poly(N-Isopropylacrylamide) and Poly(2-(Dimethylamino)Ethyl Methacrylate) Grafted on an Ordered Mesoporous Silica Surface Using Atom Transfer Radical Polymerization with Activators Regenerated by Electron Transfer. *J. Mater. Chem.* **2012**, *22* (14), 6939–6946.
24. Daoud, M.; Cotton, J. P. Star Shaped Polymers: A Model for the Conformation and Its Concentration Dependence. *J. Phys. France* **1982**, *43* (3), 531–538.
25. Ohno, K.; Morinaga, T.; Takeno, S.; Tsujii, Y.; Fukuda, T. Suspensions of Silica Particles Grafted with Concentrated Polymer Brush: Effects of Graft Chain Length on Brush Layer Thickness and Colloidal Crystallization. *Macromolecules* **2007**, *40* (25), 9143–9150.
26. Choi, J.; Hui, C. M.; Pietrasik, J.; Dong, H.; Matyjaszewski, K.; Bockstaller, M. R. Toughening Fragile Matter: Mechanical Properties of Particle Solids Assembled from Polymer-Grafted Hybrid Particles Synthesized by ATRP. *Soft Matter* **2012**, *8* (15), 4072–4082.
27. de Groot, G. W.; Santonicola, M. G.; Sugihara, K.; Zambelli, T.; Reimhult, E.; Vörös, J.; Vancso, G. J. Switching Transport through Nanopores with pH-Responsive Polymer Brushes for Controlled Ion Permeability. *ACS Appl. Mater. Interfaces* **2013**, *5* (4), 1400–1407.
28. Dong, Z.; Wei, H.; Mao, J.; Wang, D.; Yang, M.; Bo, S.; Ji, X. Synthesis and Responsive Behavior of Poly(N,N-Dimethylaminoethyl Methacrylate) Brushes Grafted on Silica Nanoparticles and Their Quaternized Derivatives. *Polymer* **2012**, *53* (10), 2074–2084.
29. Bütün, V. U. R. A. L.; Armes, S. P.; Billingham, N. C. Synthesis and Aqueous Solution Properties of near-Monodisperse Tertiary Amine Methacrylate Homopolymers and Diblock Copolymers. *Polymer* **2001**, *42* (14), 5993–6008.
30. Hampu, N.; Werber, J. R.; Chan, W. Y.; Feinberg, E. C.; Hillmyer, M. A. Next-Generation Ultrafiltration Membranes Enabled by Block Polymers. *ACS Nano* **2020**, *14* (12), 16446–16471.
31. White, E. V.; Golden, K. M.; Zharov, I.; Fullwood, D. T. Maximum Radius Percolation Path Analysis for Estimates of Particle Pass-Through Size of Nanosphere Membranes. *Phys. Rev. E* **2019**, *99*, 022904.
32. Ozgumus, T.; Mobedi, M.; Ozkol, U. Determination of Kozeny Constant Based on Porosity and Pore to Throat Size Ratio in Porous Medium with Rectangular Rods *Eng. Appl. Comput. Fluid Mech.* **2014**, *8* (2), 308–318.
33. Rogers, B. J.; Wirth, M. J. Slip Flow through Colloidal Crystals of Varying Particle Diameter. *ACS Nano* **2013**, *7* (1), 725–731.
34. Choi, C.-H.; Westin, K. J. A.; Breuer, K. S. Apparent Slip Flows in Hydrophilic and Hydrophobic Microchannels. *Physics of Fluids* **2003**, *15* (10), 2897–2902.
35. Wu, Z.; Wei, B.; Zhang, X.; Wirth, M. Efficient Separations of Intact Proteins Using Slip-Flow with Nano-Liquid Chromatography–Mass Spectrometry. J. *Anal. Chem.* **2014**, *86* (3), 1592–1598.
36. Eijkel, J. C. T.; Berg, A. van den. Nanofluidics: What Is It and What Can We Expect from It? *Microfluid Nanofluid* **2005**, *1* (3), 249–267.
37. Velasco, R.; Pathak, M.; Panja, P.; Deo, M. In *Proceedings of the 5th Unconventional Resources Technology Conference*; American Association of Petroleum Geologists: Tulsa, OK, USA, 2017.
38. Schepelina, O.; Zharov, I. Poly(2-(dimethylamino)ethyl methacrylate)-Modified Nanoporous Colloidal Films with pH and Ion Response. *Langmuir* **2008**, *24* (24), 14188–14194.
39. Daniels, C. R.; Tauzin, L. J.; Foster, E.; Advincula, R. C.; Landes, C. F. On the pH-Responsive, Charge-Selective, Polymer-Brush-Mediated Transport Probed by Traditional and Scanning Fluorescence Correlation Spectroscopy. *J. Phys. Chem. B* **2013**, *117* (16), 4284–4290.
40. Dong, Z.; Mao, J.; Wang, D.; Yang, M.; Ji, X. Synthesis and Multi-Stimuli-Responsive Behavior of Poly(N,N-Dimethylaminoethyl Methacrylate) Spherical Brushes under Different Modes of Confinement in Solution. *Langmuir* **2015**, *31* (32), 8930–8939.

# Table of Contents Graphic